Article

Cell Chemical Biology

Optogenetic Delineation of Receptor Tyrosine Kinase Subcircuits in PC12 Cell Differentiation

Graphical Abstract

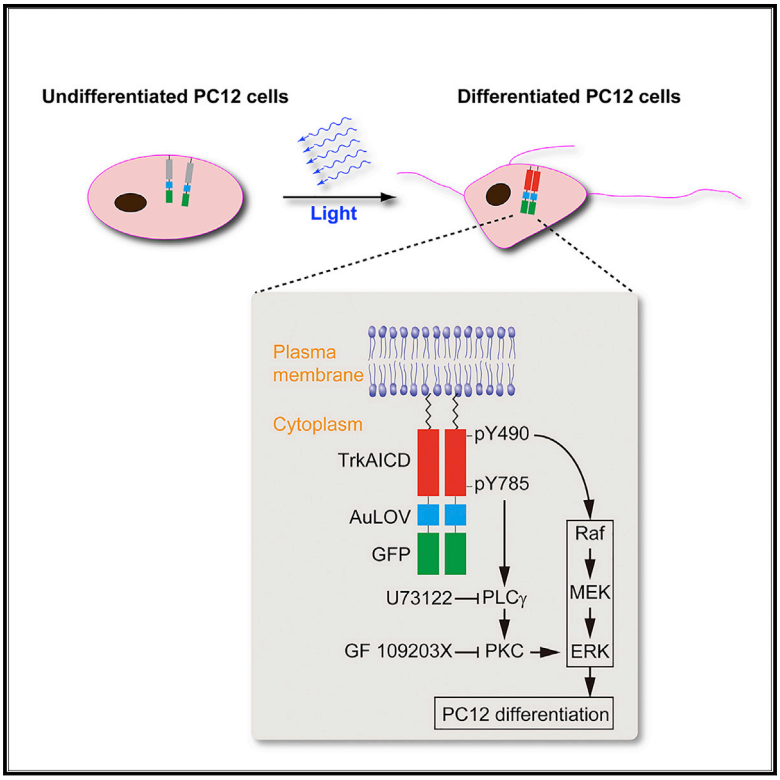

Highlights

- Non-neuronal optogenetics allows for the control of receptor tyrosine kinase activity
- Tyrosine 490 of TrkA directly activates the ERK signaling pathway
- Tyrosine 785 of TrkA activates ERK signaling through the PLCγ-PKC pathway
- Tyrosines 490 and 785 of TrkA both contribute to PC12 cell differentiation

Authors

John S. Khamo, Vishnu V. Krishnamurthy, Qixin Chen, Jiajie Diao, Kai Zhang

Correspondence

jiajie.diao@uc.edu (J.D.), kaizkaiz@illinois.edu (K.Z.)

In Brief

Khamo et al. developed a non-neuronal optogenetic system to activate TrkA signaling using blue light. In combination with pharmacological inhibition, the authors delineate the signaling role of key physiological tyrosines in the TrkA intracellular domain. Tyrosines 490 and 785 both induce PC12 cell differentiation through the ERK signaling pathway.

Khamo et al., 2019, Cell Chemical Biology *26*, 1–11
March 21, 2019
https://doi.org/10.1016/j.chembiol.2018.11.004

CellPress

Please cite this article in press as: Khamo et al., Optogenetic Delineation of Receptor Tyrosine Kinase Subcircuits in PC12 Cell Differentiation, Cell Chemical Biology (2018), https://doi.org/10.1016/j.chembiol.2018.11.004

Cell Chemical Biology
Article

Optogenetic Delineation of Receptor Tyrosine Kinase Subcircuits in PC12 Cell Differentiation

John S. Khamo,[1] Vishnu V. Krishnamurthy,[1] Qixin Chen,[4] Jiajie Diao,[4,*] and Kai Zhang[1,2,3,5,*]
[1]Department of Biochemistry, University of Illinois at Urbana-Champaign, Urbana, IL 61801, USA
[2]Neuroscience Program, University of Illinois at Urbana-Champaign, Urbana, IL 61801, USA
[3]Center for Biophysics and Quantitative Biology, University of Illinois at Urbana-Champaign, Urbana, IL 61801, USA
[4]Department of Cancer Biology, University of Cincinnati College of Medicine, Cincinnati, OH 45267, USA
[5]Lead Contact
*Correspondence: jiajie.diao@uc.edu (J.D.), kaizkaiz@illinois.edu (K.Z.)
https://doi.org/10.1016/j.chembiol.2018.11.004

SUMMARY

Nerve growth factor elicits signaling outcomes by interacting with both its high-affinity receptor, TrkA, and its low-affinity receptor, p75NTR. Although these two receptors can regulate distinct cellular outcomes, they both activate the extracellular-signal-regulated kinase pathway upon nerve growth factor stimulation. To delineate TrkA subcircuits in PC12 cell differentiation, we developed an optogenetic system whereby light was used to specifically activate TrkA signaling in the absence of nerve growth factor. By using tyrosine mutants of the optogenetic TrkA in combination with pathway-specific pharmacological inhibition, we find that Y490 and Y785 each contributes to PC12 cell differentiation through the extracellular-signal-regulated kinase pathway in an additive manner. Optogenetic activation of TrkA eliminates the confounding effect of p75NTR and other potential off-target effects of the ligand. This approach can be generalized for the mechanistic study of other receptor-mediated signaling pathways.

INTRODUCTION

The dimeric secretory nerve growth factor (NGF), the first discovered neurotrophin, exerts a broad spectrum of neuronal functions including cell survival, growth, differentiation (Chao, 2003), tissue regeneration (Widenfalk et al., 2001), pain (Hirose et al., 2016), synaptogenesis, and synaptic plasticity (Poo, 2001). Trophic effects of NGF result from its interaction with the high-affinity receptor tropomyosin receptor kinase A (TrkA) (Huang and Reichardt, 2001). Upon binding to NGF, TrkA undergoes autophosphorylation of specific tyrosines in its intracellular domain (ICD). Phosphorylated tyrosines in the TrkA ICD serve as docking sites for distinct downstream effectors to activate canonical downstream signaling pathways including the extracellular-signal-regulated kinase (ERK) and phospholipase C-γ (PLCγ) pathways (Segal, 2003).

Outcomes of TrkA signaling have been complicated, however, by the discovery that NGF also binds to its low-affinity receptor, p75NTR (Deshmukh and Johnson, 1997). In fact, p75NTR binds to other neurotrophins including brain-derived neurotrophic factor, neurotrophin-3, and neurotrophin-4/5 with similar affinities (Bothwell, 1995). Evidence suggests a 2-fold neuronal function of p75NTR: (1) it can functionally collaborate with TrkA to enhance neurotrophin binding and receptor activation (Barker, 1998; Dechant and Barde, 2002), and (2) it can also induce cell apoptosis via ProNGF-dependent signaling processes (Lee et al., 2001). Although NGF stimulation leads to ERK phosphorylation primarily through its binding to TrkA, ERK activation can also be mediated by p75NTR (Susen et al., 1999). Thus, the existence of multiple receptors for NGF makes it challenging to delineate specific roles of TrkA subcircuits in the biological context (Chao, 2003; Lu et al., 2005).

In vitro and *in vivo* models have been developed to delineate the sole contributions of TrkA and p75NTR to NGF signaling. Cell lines and transgenic animal models with either gene disrupted have been generated. For instance, the PC12nnr5 cell line expresses only p75NTR (lacking TrkA) (Green et al., 1986), while PC12-p75^{-} cells express only TrkA (lacking p75NTR) (Bassili et al., 2010). Additionally, 3T3 cells have been engineered to express TrkA or p75NTR (Huang et al., 1999). Similarly, p75NTR mutant mice (Lee et al., 1992) and TrkA knockout mice (Liebl et al., 2000) have been developed. However, caution is warranted with genetic manipulation for at least two reasons. First, complete deletion of a gene may undesirably corrupt its roles in other cellular functions. For instance, p75NTR is widely expressed in non-neuronal tissues (Lomen-Hoerth and Shooter, 1995) and is involved in processes such as liver repair (Passino et al., 2007) and muscle regeneration (Colombo et al., 2011). Second, genetic manipulation often causes delayed responses and constitutive alteration of gene expression in cells. Alternatively, pharmacological inhibition can be used to primarily target specific pathways to dissect the NGF signaling network. However, potential off-target effects should be considered (Arcaro and Wymann, 1993; Liu et al., 2005; Martin et al., 2011).

Even at the level of TrkA, contradictory evidence exists with respect to the functionality of its downstream subcircuits. Upon phosphorylation, two tyrosine residues, Y490 and Y785, serve as primary docking sites for downstream effectors. Y490

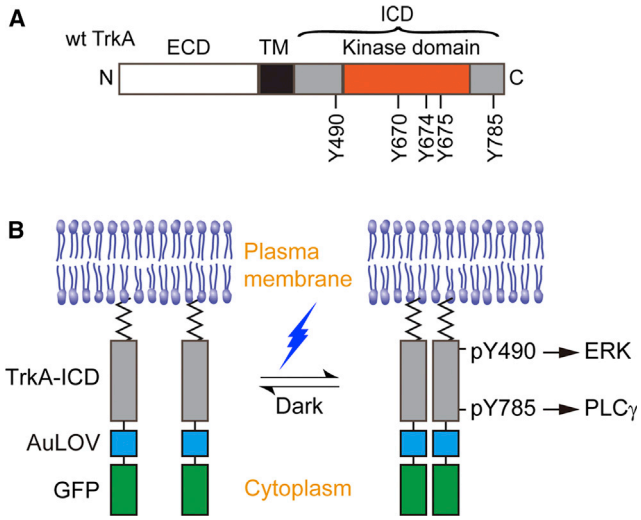

Figure 1. Design of the Optogenetic TrkA System

(A) Representation of the wild-type (wt) TrkA receptor. TrkA is a type I transmembrane protein anchored at the plasma membrane by a single-helix transmembrane domain (TM). Nerve growth factor associates with the extracellular domain (ECD) to promote receptor dimerization and phosphorylation of key tyrosines within the intracellular domain (ICD). Y670, Y674, and Y675 are critical for kinase activity, while Y490 and Y785 are involved in the initiation of the Raf/MEK/ERK and PLCγ-PKC signaling pathways, respectively.

(B) Schematic representation of the optogenetic TrkA receptor. The ECD and TM are replaced by a lipidation motif to abolish ligand sensitivity, while retaining normal orientation and localization at the plasma membrane. Light sensitivity is introduced through fusion with the photosensitive protein, AuLOV. Illumination with blue light should promote dimerization of receptor ICDs and activation of downstream signaling pathways. GFP serves as a probe for system expression.

associates with Shc and Src domains (Stephens et al., 1994), which further activate the Raf/MEK/ERK signaling pathway, whereas Y785 associates with PLCγ (Figure 1). Work based on a chimeric receptor, a fusion protein of the platelet-derived growth factor (PDGF) receptor extracellular domain (ECD) and TrkA ICD, shows that the mutation of Y785 in TrkA, which is believed to primarily activate the PLCγ signaling pathway, does not affect PC12 cell differentiation (Obermeier et al., 1994). However, overexpression of the Src Homology domains of PLCγ1 inhibits NGF-induced PC12 cell differentiation (Bae et al., 1998), presumably through competition with endogenous PLCγ for receptor interaction. This discrepancy can arise from unknown off-target effects of the ligand or overexpressed protein domains, both of which are challenging to analyze quantitatively. Thus, delineation of TrkA subcircuits calls for the development of new strategies that can evaluate the functionality of specific tyrosines of the TrkA ICD with a clean biological context free from potential off-targets.

The emerging optogenetic techniques provide a new way to study signaling mechanisms by integrating photoactivatable proteins with signaling molecules (Khamo et al., 2017; Kim and Lin, 2013; Muller et al., 2014; Tischer and Weiner, 2014; Toettcher et al., 2011; Tucker, 2012; Zhang and Cui, 2015; Zoltowski and Gardner, 2011). As light can be easily manipulated with high spatial and temporal resolution, optogenetic control of signaling can provide insights into the kinetic and spatial features of signal transduction. In addition, light can bypass ligand binding to specifically interrogate optogenetically engineered receptors, whose ligand can interact with and signal through multiple known and potentially unidentified receptors.

Here, we use an optogenetic approach to specifically elucidate the signaling outcomes of TrkA subcircuits in the absence of NGF. By constructing wild-type and tyrosine mutants of the optogenetic TrkA receptor, we control canonical TrkA signaling without introducing a ligand-based chimeric receptor or disturbing the endogenous TrkA expression and function. We find that both Y490 and Y785 of TrkA regulate PC12 cell differentiation, with Y490 primarily activating the ERK pathway and Y785 contributing to the ERK signaling cascade in a PLCγ- and PKC-dependent manner.

RESULTS

System Construction

Natural signal transduction mediated by TrkA sequentially involves NGF interaction with the receptor ECD, receptor dimerization, and a series of autophosphorylation at key tyrosines throughout the receptor ICD (Figure 1A). Several tyrosines located within the receptor kinase domain are critical for optimal kinase activity, and some tyrosines located outside of the kinase domain serve as docking sites for initiating factors of intracellular signaling pathways. To bypass the ligand requirement for receptor activity, we constructed an optogenetic TrkA (Lyn-TrkAICD-AuLOV-GFP) by fusing a homo-associating domain, the light-oxygen-voltage domain of aureochrome1 from *Vaucheria frigida* (AuLOV) (Grusch et al., 2014), to the ICD of the wild-type TrkA receptor (Figure 1B). This construct will be referred to as "WT ICD." Lyn is the lipidation motif of the Src family Lyn kinase, which serves as a membrane-targeting peptide that replaces the transmembrane and extracellular domain of TrkA. This construct is different from a previously reported optogenetic TrkA system, which used the full-length TrkA fused to the photoactivatable protein, cryptochrome 2 (Chang et al., 2014). We chose to control TrkA ICD alone to avoid the potential interaction of TrkA ECD with other receptors such as p75NTR (Covaceuszach et al., 2015), although this interaction is a subject of debate (Wehrman et al., 2007). For practical convenience, we chose AuLOV because of its smaller size (145 amino acids) compared with cryptochrome 2 (498 amino acids). In our system, we expected that light-induced homo-association of AuLOV would bring TrkA kinase domains within proximity of each other to initiate the cross- and autophosphorylation of specific tyrosines throughout the ICDs, including Y490 and Y785. To delineate the signaling outcomes of these two docking sites, we also constructed single tyrosine-to-phenylalanine mutants (Y490F, Y785F) and a double mutant (Y490/785F) of WT ICD. Note that light-induced activation of the optogenetic TrkA system should not activate the endogenous wild-type TrkA.

Blue-Light Illumination Induces Homo-Association of Optogenetic TrkA in Live Cells

When overexpressed in PC12 cells, WT ICD and its mutant variants localized primarily on the plasma membrane (Figure 2A). Compared with a cytosolic GFP, optogenetic TrkA variants

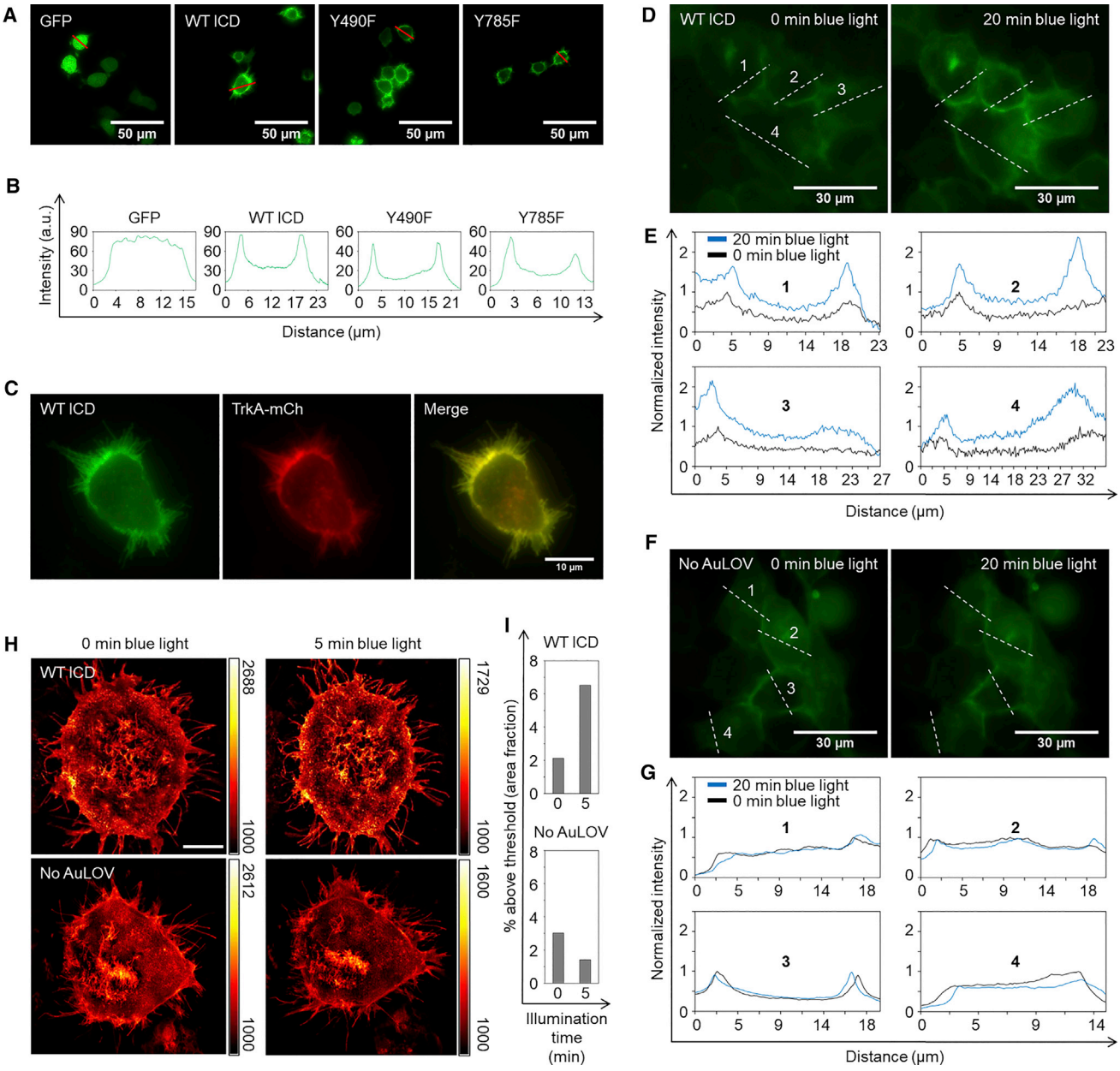

Figure 2. Optogenetic TrkA Localizes to the Plasma Membrane and Homo-Associates in Response to Blue Light

(A) Fluorescence microscopy images of PC12 cells expressing a cytosolic GFP or variants of the optogenetic TrkA system.

(B) Red-line profile analysis of fluorescence images in (A) reveals a strong membrane localization of the optogenetic constructs.

(C) Overexpression of wild-type (WT) ICD and TrkA-mCherry shows that both fusion proteins primarily localize to the plasma membrane.

(D) BiFC assay based on split Venus fragments. A 20-min blue-light illumination (5 mW/cm^2) increased the fluorescence intensity in cells co-transfected with Lyn-TrkAICD-AuLOV-VN and Lyn-TrkAICD-AuLOV-VC. Images of the same cells were acquired before and after blue-light treatment.

(E) Intensity quantification along four dashed-line profiles outlined in (D).

(F and G) Same as (D) and (E) except that a No AuLOV control, Lyn-TrkAICD-VN and Lyn-TrkAICD-VC, is used. The same blue-light illumination does not enhance the fluorescence intensity.

(H) Structured illumination microscopy (SIM) images of MDA-MB-231 cells expressing WT ICD (top panels) or No AuLOV control (bottom panels) before and after blue-light (405 nm) irradiation. Scale bar, 10 μm.

(I) Quantification of the fraction of images whose intensity is above a threshold set at 50% of the maximum intensity of the background-subtracted images. Data shown in (D) to (G) are representative of more than 500 cells (N > 500) from two biological replicates (n = 2). Data shown in (H) and (I) represent WT ICD (N = 4) and No AuLOV (N = 3) from two biological replicates (n = 2). See also Figure S1.

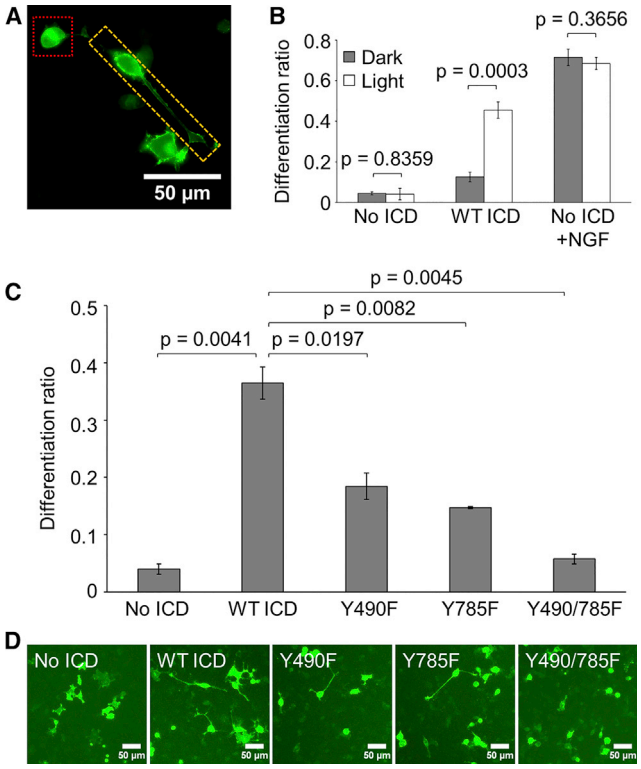

Figure 3. Optogenetic TrkA Promotes PC12 Cell Differentiation in Response to Blue-Light Stimulation

(A) Image for reference depicting differentiated (yellow box) and undifferentiated (red box) PC12 cells transfected with No ICD and treated with 50 ng/mL NGF for 24 hr.

(B) Differentiation ratios calculated for PC12 cells expressing wild-type (WT) ICD or No ICD. Transfected cells were illuminated with 300 $\mu W/cm^2$ blue light or kept in the dark for 44 hr prior to imaging. WT ICD mediated significant light-induced differentiation compared with No ICD. Cells expressing No ICD in the presence of 50 ng/mL NGF underwent robust differentiation in a light-independent manner. Values represent the mean ± SD of three biological replicates (n = 3) with >70 cells counted per replicate.

(C) Differentiation ratios calculated for PC12 cells expressing variants of the optogenetic TrkA system. Transfected cells were illuminated with 300 $\mu W/cm^2$ blue light for 24 hr prior to imaging. Y490F and Y785F showed a significant reduction in light-induced differentiation compared with WT ICD. Y490/785F resulted in a differentiation ratio similar to that of No ICD. Values represent the mean ± SD of two biological replicates (n = 2) with >900 cells counted per replicate.

(D) Representative fluorescence images of the conditions reported in (C). Scale bars, 50 µm.

showed higher fluorescence intensity at the plasma membrane relative to the cytoplasm (Figure 2B). In the absence of ligand binding, the plasma membrane is the main subcellular localization of wild-type TrkA in PC12 cells, which was revealed in previous work by crosslinking NGF with wild-type TrkA (Hartman et al., 1992) as well as immunostaining of TrkA (Grimes et al., 1996). In addition, overexpression of fluorescently labeled TrkA results in primary targeting to the plasma membrane (Wang et al., 2011; Zhang et al., 2013). Here, we reproduced the results of TrkA overexpression and found that TrkA-mCherry overlapped with WT ICD in PC12 cells (Figure 2C), suggesting that the Lyn sequence allows for subcellular localization of TrkA ICD to the natural membrane compartment of full-length TrkA.

To confirm that blue light could induce the homo-association of WT ICD, we performed a bimolecular fluorescence complementation (BiFC) assay based on split Venus fragments, VN (amino acids 1–154) and VC (amino acids 155–238) (Saka et al., 2007; Shyu et al., 2006). Two plasmids were constructed: Lyn-TrkAICD-AuLOV-VN and Lyn-TrkAICD-AuLOV-VC. As expected, after 20 min of blue-light illumination, fluorescence intensity from cells co-transfected with both plasmids increased (Figures 2D and 2E). In cells co-transfected with the No AuLOV control (Lyn-TrkAICD-VN and Lyn-TrkAICD-VC), the same dose of blue light did not increase the fluorescence intensity (Figures 2F and 2G).

We also used structured illumination microscopy (SIM) to probe blue-light-induced receptor homo-association. MDA-MB-231 cells were transfected with WT ICD and were exposed to blue light. To quantify the light-induced homo-association of WT ICD, we analyzed the SIM images using the thresholding technique. By setting the threshold at the midpoint value between the minimal and maximal intensity of the background-subtracted cell images, we calculated the percentage of above-threshold regions over the whole cell area using ImageJ based on a published protocol (Jensen, 2013). Following 5 min of blue-light (405 nm) illumination, the above-threshold percentage increased in cells transfected with WT ICD, in stark contrast to cells transfected with the No AuLOV control (Lyn-TrkAICD-GFP), which showed no increase in the above-threshold percentage (Figures 2H and 2I).

In addition to microscopy, we were inspired by a previous optogenetic study (Zhou et al., 2012) to use native PAGE to resolve the light response of AuLOV. Cells were transfected with WT ICD and lysates were harvested in 0.5% Triton X-100 in PBS. Lysates were treated with blue light (5 mW/cm^2) for 5 min or kept in the dark. Equal amounts of each lysate were loaded on a native gel. The lane containing the illuminated sample underwent continued exposure to blue light throughout the electrophoresis. Samples were then analyzed by western blot using an anti-GFP antibody. As expected, blue light resulted in a reduced mobility shift of the most prominent band in the dark control, indicative of light-mediated homo-association (Figure S1).

Light-Induced Activation of Optogenetic TrkA Results in PC12 Cell Differentiation

PC12 cells project neurites in response to NGF stimulation, a process referred to as differentiation (Figure 3A). We proceeded to determine whether WT ICD activation could achieve a similar cellular outcome. PC12 cells transfected with WT ICD were exposed to blue light (300 $\mu W/cm^2$) for 2 days in a humidified 37°C CO_2 incubator before their fluorescence images were acquired. Light stimulation of these cells resulted in significant differentiation (45%) compared with cells kept in the dark (12%) (Figure 3B). Cells expressing the optogenetic construct without the TrkA ICD (No ICD) showed little differentiation in both light and dark (<5%), indicating that light-induced differentiation was ICD-dependent. Cells expressing No ICD showed robust differentiation (>68%) when treated with 50 ng/mL NGF, indicating that endogenous TrkA retained ligand sensitivity and signaling activity.

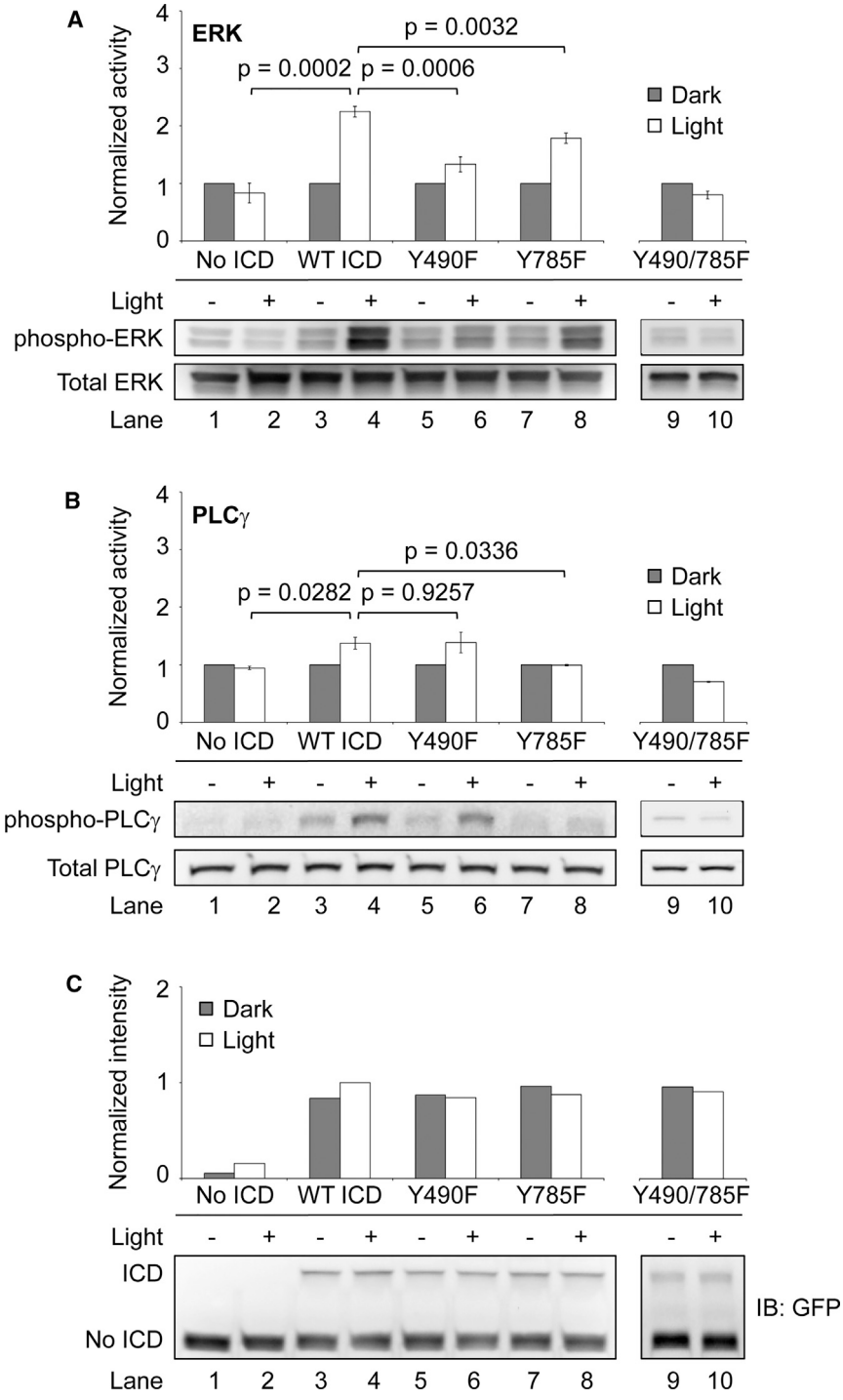

Figure 4. Light-Induced Optogenetic TrkA Mutants Differentially Activate the ERK and PLCγ Pathways

(A and B) Western blot analysis of light-induced (A) ERK and (B) PLCγ activity exhibited by PC12 cells expressing variants of the optogenetic TrkA system. Transfected cells were serum-starved overnight following transfection, and were illuminated with 5 mW/cm^2 blue light or kept in the dark for 10 min prior to lysis. Compared with wild-type (WT) ICD, Y490F displayed a dramatic reduction in ERK activity with no change in PLCγ activity. Y785F showed a relatively modest reduction in ERK activity with nearly abrogated PLCγ activity. Y490/785F showed no light-induced activity for either pathway, similar to No ICD. Values represent the mean ± SD of three separate experiments (n = 3) for ERK and two separate experiments (n = 2) for PLCγ. (C) Western blot analysis of system expression by probing GFP. Expression level across samples fluctuates within 16%.

Light-Induced Activation of Optogenetic TrkA Mutants Results in Diminished PC12 Cell Differentiation

To determine the functional role of Y490 and Y785 in differentiation, we transfected PC12 cells with mutant constructs and illuminated them for 24 hr as previously described. Cells expressing Y490F or Y785F exhibited significantly reduced levels of light-induced differentiation (18% or 15%, respectively) compared with cells expressing WT ICD (36%) (Figures 3C and 3D). Furthermore, the degree of differentiation undergone by cells expressing Y490/785F (6%) was similar to that displayed by cells expressing No ICD (4%), suggesting that Y490 and Y785 each contributed to TrkA-mediated PC12 cell differentiation.

Light-Induced Optogenetic TrkA Mutants Differentially Activate the ERK and PLCγ Pathways

To interrogate the mechanism behind the reduced differentiation mediated by the optogenetic TrkA mutants, we performed western blots to probe the activity of downstream signaling pathways. To minimize baseline signaling activity and capture subtle differences between conditions, we transfected PC12 cells with mixtures of the variant ICD constructs and the No ICD construct. Cells were illuminated for 10 min with 5 mW/cm^2 blue light prior to lysis. Both Y490F and Y785F showed a significant reduction in ERK signaling compared with WT ICD, with the reduction for Y490F being more pronounced (Figure 4A, lanes 4, 6, and 8). Cells expressing Y490F showed no change in light-induced PLCγ activity compared with WT ICD, while Y785F showed a complete loss of PLCγ activity (Figure 4B, lanes 4, 6, and 8). These results indicate that Y490 primarily contributed to ERK activity while Y785 primarily contributed to PLCγ activity. Additionally, Y785 seemed to partially contribute to ERK signaling as evidenced by the residual ERK activity observed for Y490F (Figure 4A, lane 6) and the reduction in ERK activity observed for Y785F (Figure 4A, lane 8) compared with WT ICD. To confirm that the observed variations in signaling were a result of specific mutations and not

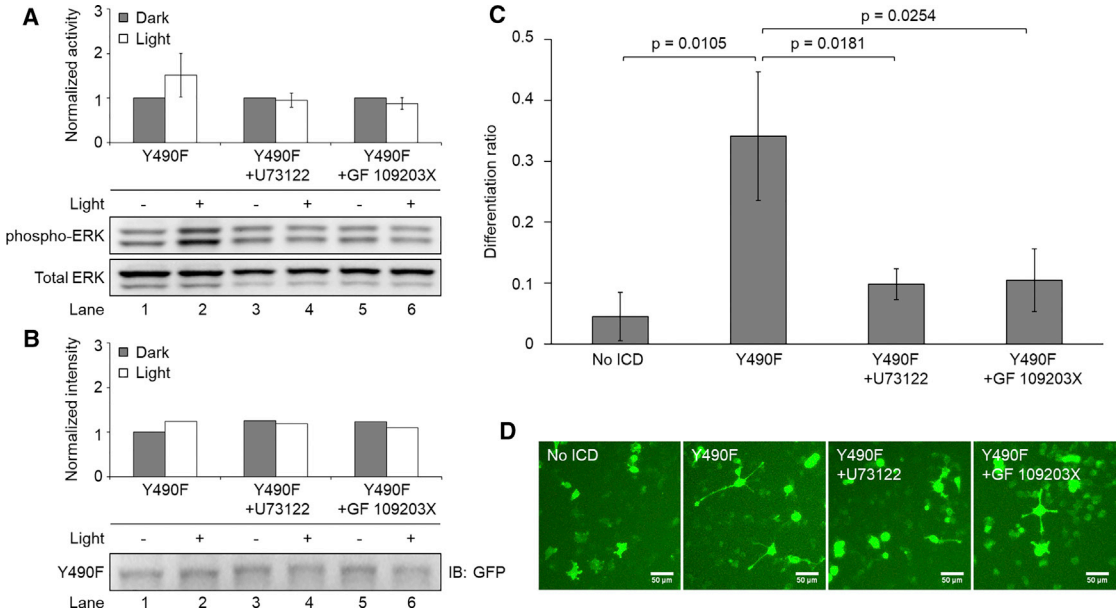

Figure 5. Y490F-Mediated ERK Signaling Is Abolished by PLCγ-PKC Inhibitors

(A) Western blot analysis of light-induced ERK activity exhibited by PC12 cells expressing Y490F. Transfected cells were serum-starved overnight following transfection and were treated with a PLCγ inhibitor (U73122, 1 μM) or a PKC inhibitor (GF 109203X, 1 μM) for 10 min prior to illumination. Cells were subsequently illuminated with 5 mW/cm^2 blue light or kept in the dark for 10 min prior to lysis. Cells treated with U73122 or GF 109203X had abolished light-induced ERK activity compared with the untreated control. Values represent the mean ± SD of two separate experiments (n = 2) for untreated and four separate experiments (n = 4) for U73122 and GF 109203X.

(B) Western blot analysis of system expression by probing GFP. The expression level for illuminated conditions fluctuates within 14%.

(C) Differentiation ratios calculated for PC12 cells expressing Y490F in the presence of U73122 (1 μM) or GF 109203X (1 μM). Inhibitors were added to cells 1 hr prior to illumination. Cells were illuminated with 300 μW/cm^2 blue light for 24 hr prior to imaging. Cells treated with U73122 or GF 109203X had decreased light-induced differentiation compared with the untreated control, which received inhibitor vehicle (DMSO). Values represent the mean ± SD of three biological replicates (n = 3) with >40 cells counted per replicate.

(D) Representative fluorescence images of the conditions reported in (C). Scale bars, 50 μm.

due to significant variability in system expression, we probed lysates with an anti-GFP antibody. All constructs were expressed at a comparable level (Figure 4C).

Y785 Contributes to ERK Signaling and PC12 Cell Differentiation in a PLCγ-PKC-Dependent Manner

Given that Y785 is essential for PLCγ activity, we speculated that the contribution of Y785 to ERK signaling was mediated by pathway crosstalk. Indeed, findings from previous studies support this notion (Mauro et al., 2002; Ueda et al., 1996). To validate this, we transfected PC12 cells as previously described with a combination of Y490F and No ICD. Transfected cells were then treated with a PLCγ inhibitor (U73122, 1 μM) or a PKC inhibitor (GF 109203X, 1 μM) 10 min prior to illumination. With the inhibitors still present, cells were then illuminated for 10 min with 5 mW/cm^2 blue light before lysis and subsequent immunoblotting (Figure 5A). Compared with untreated cultures, all cells treated with inhibitors displayed an abrogation of the light-induced residual ERK activity mediated by Y490F (Figure 5A, lanes 2, 4, and 6), suggesting that the role of Y785 in ERK signaling is dependent on the PLCγ-PKC pathway. To confirm that the observed variations in signaling were not due to significant variability in system expression, we probed lysates with an anti-GFP antibody. All constructs were expressed at a comparable level (Figure 5B). In addition to interrogating the short-term effect of inhibitors on light-induced ERK signaling mediated by Y490F, we set out to determine the effect of long-term inhibition on PC12 cell differentiation. PC12 cells overexpressing Y490F were illuminated with blue light (300 μW/cm^2) for 24 hr in the presence or absence of U73122 (1 μM) or GF 109203X (1 μM). Inhibitors were added 1 hr prior to illumination. Cell cultures treated with either inhibitor showed significantly reduced differentiation, suggesting that Y785 also contributes to PC12 cell differentiation in a PLCγ-PKC-dependent manner (Figures 5C and 5D).

DISCUSSION

We developed an optogenetic TrkA system to study differentiation in PC12 cells by photoactivation of the TrkA ICD and its downstream signaling pathways. Light-mediated homo-association of TrkA resulted in elevated ERK and PLCγ activity. Light stimulation specifically activated the optogenetic TrkA, efficiently decoupling its signaling from endogenous TrkA and p75NTR. By generating mutants of the signal pathway-specific tyrosines, Y490 and Y785, we used this system to determine the mechanisms by which TrkA regulates PC12 cell differentiation. In a previous study, we demonstrated that optogenetic activation of Raf/MEK/ERK signaling is sufficient to induce PC12 cell differentiation, suggesting that this pathway is a strong

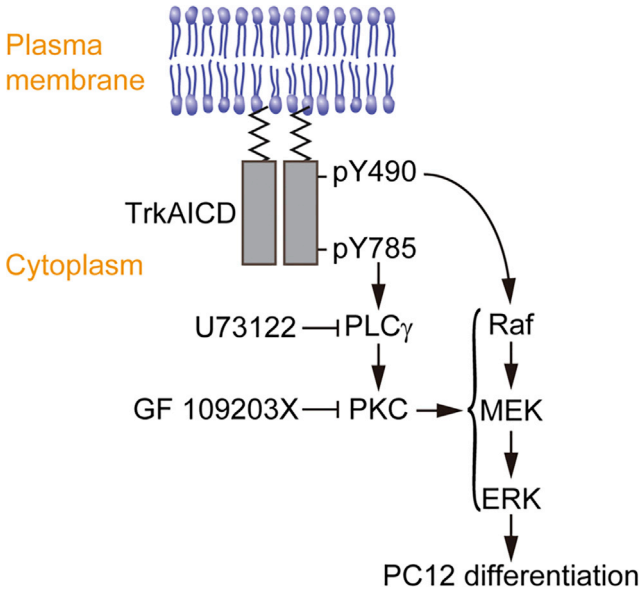

Figure 6. Proposed Model for the Role of Y490 and Y785 in TrkA-Mediated PC12 Cell Differentiation

The Raf/MEK/ERK signaling cascade, primarily instigated by Y490 of TrkA, is essential for PC12 cell differentiation. Y785 instigates the PLCγ-PKC pathway, which feeds into the Raf/MEK/ERK signaling cascade. Mutating Y785 or inhibiting the PLCγ-PKC pathway results in diminished receptor-mediated ERK signaling and differentiation in PC12 cells.

correlating factor for the phenotype (Krishnamurthy et al., 2016). From our experiments employing optogenetic TrkA mutants in combination with pathway-specific inhibitors, we propose a model of the TrkA signaling network in the context of PC12 cell differentiation (Figure 6). We find that Y490 regulates ERK signaling and Y785 primarily regulates PLCγ signaling. Y785 also promotes ERK signaling in a PLCγ-PKC-dependent manner. Indeed, previous studies showed that PKC could feed into the Raf/MEK/ERK signaling cascade (Mauro et al., 2002; Ueda et al., 1996). The reduced differentiation caused by the Y490F and Y785F single mutants, and the abolished differentiation observed for the Y490/785F double mutant, suggest that TrkA uses both Y490 and Y785 to activate Raf/MEK/ERK signaling to promote PC12 cell differentiation.

Based on previous studies (Obermeier et al., 1994; Stephens et al., 1994), PC12 cells expressing the Y490/785F double mutant did not differentiate in the presence of NGF, in agreement with our optogenetic result. However, the individual contribution of Y490 and Y785 to PC12 cell differentiation has been elusive. In one case, expression of single mutants Y490F and Y785F did not affect NGF-induced PC12 cell differentiation, suggesting redundancy in their phenotypical role (Stephens et al., 1994). In the other case, Y490F resulted in a dramatic loss of differentiation while Y785F had no effect (Obermeier et al., 1994). This discrepancy may be due to the nature of the ligands (i.e., NGF versus PDGF) used in these studies.

Using our optogenetic TrkA system, we show that Y490 and Y785 make significant and additive contributions to PC12 cell differentiation. We found that Y490F and Y785F each diminished PC12 cell differentiation to approximately half of that promoted by WT ICD (Figure 3C). A similar additive trend was observed for their capacity to activate ERK (Figure 4A). Stephens et al. (1994) observed a similar reduction of ERK activity for both Y490F and Y785F compared with wild-type TrkA. At the phenotypic level, however, Y490F and Y785F promoted a degree of PC12 cell differentiation comparable with that promoted by wild-type TrkA. These results indicate that an ERK signaling threshold exists for establishing maximal differentiation. It is possible that this threshold was exceeded by both Y490F and Y785F when stimulated with NGF. Here, we note that PC12 cell differentiation mediated by WT ICD was less than that of NGF treatment (Figure 3B). We speculated that this was a result of a difference in signaling intensity between ligand- and light-simulated receptors. To test this idea, we compared the ERK activity induced by WT ICD (Figure 7A) with NGF treatment (Figure 7B). Given that not all cells are light-responsive in transfected cultures, we defined the signaling response of optogenetic TrkA as $S_{\text{optoTrkA}} = \frac{\text{R(light, WT ICD)} - \text{R(light, No ICD)}}{\text{R(dark, WT ICD)} - \text{R(dark, No ICD)}}$. We defined the NGF signaling response of untransfected cells as $S_{\text{NGF}} = \frac{\text{R(NGF)}}{\text{R(No NGF)}}$. R is the signal ratio of phosphorylated ERK over total ERK probed by western blot. Figures 7A and 7B show that light elicited a milder signaling response ($S_{\text{optoTrkA}} = 6.2$) compared with NGF treatment ($S_{\text{NGF}} = 9.2$). This result suggests that NGF elicits higher ERK activity than WT ICD, at least on a short timescale (5–10 min). To determine whether a similar signaling difference exists at a longer timescale, we compared the ERK activity generated by NGF and light-activated WT ICD after 4 hr and 24 hr of treatment. As expected, NGF promoted higher ERK activity than WT ICD at both time points (Figure 7C).

Thus, the previously observed reduction of ERK activity for NGF-treated PC12 cells expressing either Y490F or Y785F may still surpass the signaling threshold required for saturated differentiation, thereby obscuring the contribution of individual tyrosines (Stephens et al., 1994). On the other hand, the optogenetic Y490F and Y785F likely produce a subthreshold ERK activity when stimulated with light, providing advantages in interpreting the phenotypic role of each tyrosine. These results suggest that the difference between light- and ligand-induced PC12 cell differentiation resulted from their distinct potency in the induction of ERK signaling, the reason for which has yet to be determined, although it can be speculated that p75NTR plays a role in the presence of the ligand. In the physiological context, while Y490 primarily mediates the ERK-dependent trophic effects of NGF, we speculate that the role of Y785 in ERK signaling becomes more critical when NGF concentrations are low.

Finally, we asked whether pharmacological inhibition of NGF-induced PLCγ-PKC activity would support our proposed model of the TrkA signaling network in the context of PC12 cell differentiation. We performed a differentiation assay in the presence of U73122 or GF 109203X. As expected, NGF-induced differentiation was reduced by both inhibitors in a dose-dependent manner, supporting our previous finding that the PLCγ-PKC axis contributes to PC12 cell differentiation (Figure 7D).

Optogenetic activation of TrkA provides an attractive approach to dissect NGF signaling processes by leaving the endogenous

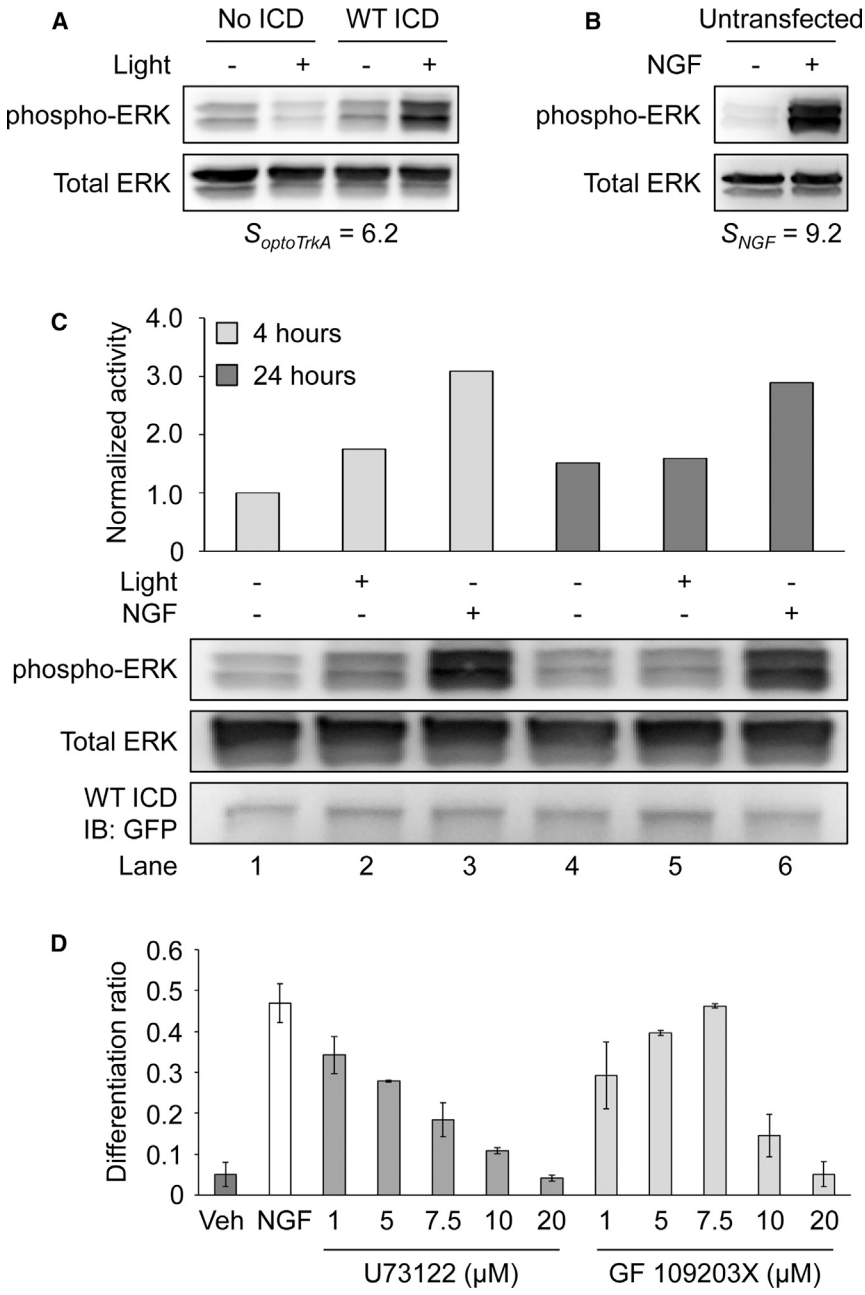

Figure 7. NGF Elicits Higher ERK Activity Compared with Optogenetic TrkA, and NGF-Mediated PC12 Cell Differentiation Is Reduced by Pharmacological Inhibition of PLCγ and PKC in a Dose-Dependent Manner

(A) Western blot analysis of two separate experiments. Transfected cells (No ICD and wild-type [WT] ICD) were serum-starved overnight following transfection. Cells were illuminated with 5 mW/cm^2 blue light or kept in the dark for 10 min prior to lysis.

(B) Untransfected cells were serum-starved overnight prior to treatment. Cells were untreated or treated with NGF (100 ng/mL) for 5 min prior to lysis. The ERK activity mediated by optogenetic TrkA was lower than that of NGF.

(C) Western blot analysis of ERK signaling mediated by long-term NGF or WT ICD activity. PC12 cells were transfected with WT ICD and serum-starved overnight following transfection. Cells were then kept in the dark, illuminated with 300 μW/cm^2 blue light, or treated with NGF (50 ng/mL) for 4 or 24 hr prior to lysis. Untreated cells received NGF vehicle (sodium acetate). NGF stimulation elicited higher ERK activity than WT ICD for both durations. All samples are normalized to lane 1.

(D) Differentiation ratios for PC12 cells treated with NGF in the presence of U73122 or GF 109203X. Serum-starved cells were treated with inhibitors (1, 5, 7.5, 10, and 20 μM) 1 hr prior to NGF treatment. Cells were treated with NGF (50 ng/mL) for 24 hr. Cells were stained with 1 μM Calcein AM 10 min before imaging. NGF-induced PC12 cell differentiation was reduced by U73122 or GF 109203X in a dose-dependent manner. Untreated cells received NGF vehicle (sodium acetate) and inhibitor vehicle (DMSO). Values represent the mean ± SD of two biological replicates (n = 2) with >400 cells counted per replicate.

TrkA expression unperturbed and by bypassing p75NTR signaling. As we have demonstrated, optogenetics can also be applied together with conventional inhibitor-based assays to further delineate signaling mechanisms. Although this work has primarily focused on delineation of TrkA signaling in mammalian cells, utilization of this optogenetic TrkA system in multicellular organisms should be applicable. Indeed, recent work from multiple laboratories including our own has demonstrated optogenetic control of intracellular signaling pathways in *Drosophila* (Guglielmi et al., 2015; Johnson et al., 2017), zebrafish (Buckley et al., 2016; Reade et al., 2016), *Xenopus* (Krishnamurthy et al., 2016), and mice (Konermann et al., 2013; Kyung et al., 2015; Lee et al., 2017; Wang et al., 2017). Notably, *in vivo* application of optogenetics has been significantly improved by the utilization of novel nanometer materials, such as upconversion nanoparticles (Chen et al., 2018; He et al., 2015; Huang et al., 2016; Zhang et al., 2016), to convert near-infrared light to visible light and facilitate deep-tissue light delivery. As receptor tyrosine kinase activation is a common function for a variety of growth factors and cytokines, we expect that this strategy can be generalized to study other receptor-mediated signal transduction pathways.

SIGNIFICANCE

Cell fate is largely determined by integrating and processing a variety of signaling inputs from the environment. To effectively and precisely transmit extracellular signals into the cell, delicate signaling machinery is required. Transmembrane receptors serve as the major machinery for transducing membrane-impermeant extracellular signals. In some cases, one type of ligand may bind to a variety of receptors to elicit distinct signaling outcomes. The signaling mechanisms of

these receptors are often confounded, particularly when common downstream signaling pathways are activated. In these cases, mechanistic delineation of the signaling mediated by each type of receptor calls for a strategy that can successfully decouple receptor activity. Nerve growth factor is one such ligand that interacts with both its high-affinity and low-affinity receptors, TrkA and p75NTR, both of which activate the extracellular-signal-regulated kinase pathway. To delineate TrkA subcircuits from those of p75NTR, we developed an optogenetic system whereby light was used to specifically activate TrkA signaling in the absence of nerve growth factor. By combining optogenetics with pharmacological assays, we demonstrated that the tyrosine residues Y490 and Y785 of the TrkA intracellular domain each contributes to PC12 cell differentiation through the extracellular-signal-regulated kinase pathway in an additive manner. Because receptor tyrosine kinase signaling is involved in neurological disorders, development, and cancer, we believe that delineating the signaling outcomes of TrkA subcircuits could lead to new insights into pathological conditions.

STAR★METHODS

Detailed methods are provided in the online version of this paper and include the following:

- KEY RESOURCES TABLE
- CONTACT FOR REAGENT AND RESOURCE SHARING
- EXPERIMENTAL MODEL AND SUBJECT DETAILS
  - Cell Culture
- METHOD DETAILS
  - Materials
  - Plasmids Construction
  - Cell Culture and Transfection
  - PC12 Cell Differentiation Assay
  - Epi-Illumination Fluorescence Live-Cell Microscopy
  - Three-Dimensional Structured Illumination Microscopy (SIM)
  - Western Blot
- QUANTIFICATION AND STATISTICAL ANALYSIS

SUPPLEMENTAL INFORMATION

Supplemental Information includes one figure and can be found with this article online at https://doi.org/10.1016/j.chembiol.2018.11.004.

ACKNOWLEDGMENTS

We thank Prof. Tobias Meyer at Stanford University for providing the PC12 cell line and Dr. Jun-Lin Guan at the University of Cincinnati for MDA-MB-231 cells. We thank Prof. Erik Procko at the University of Illinois, Urbana-Champaign for providing split Venus plasmids. We thank Dr. Sandra McMasters from the cell media facility at the University of Illinois, Urbana-Champaign for providing DH5α competent cells. K.Z. thanks the funding support from University of Illinois at Urbana-Champaign. J.D. thanks the support from National Institutes of Health (R35GM128837).

AUTHOR CONTRIBUTIONS

K.Z. and J.S.K. conceived the experiments. J.S.K., V.V.K., and Q.C. executed the experiments. J.S.K., V.V.K., Q.C., J.D., and K.Z. analyzed the data. J.S.K., J.D., and K.Z. wrote the manuscript.

DECLARATION OF INTERESTS

The authors declare no competing interests.

Received: June 9, 2018
Revised: August 13, 2018
Accepted: November 2, 2018
Published: December 27, 2018

REFERENCES

Arcaro, A., and Wymann, M.P. (1993). Wortmannin is a potent phosphatidylinositol 3-kinase inhibitor—the role of phosphatidylinositol 3,4,5-trisphosphate in neutrophil responses. Biochem. J. *296*, 297–301.

Bae, S.S., Lee, Y.H., Chang, J.S., Galadari, S.H., Kim, Y.S., Ryu, S.H., and Suh, P.G. (1998). Src homology domains of phospholipase C gamma 1 inhibit nerve growth factor-induced differentiation of PC12 cells. J. Neurochem. *71*, 178–185.

Barker, P.A. (1998). p75NTR: a study in contrasts. Cell Death Differ. *5*, 346–356.

Bassili, M., Birman, E., Schor, N.F., and Saragovi, H.U. (2010). Differential roles of Trk and p75 neurotrophin receptors in tumorigenesis and chemoresistance ex vivo and in vivo. Cancer Chemother. Pharmacol. *65*, 1047–1056.

Bothwell, M. (1995). Functional interactions of neurotrophins and neurotrophin receptors. Annu. Rev. Neurosci. *18*, 223–253.

Buckley, C.E., Moore, R.E., Reade, A., Goldberg, A.R., Weiner, O.D., and Clarke, J.D. (2016). Reversible optogenetic control of subcellular protein localization in a live vertebrate embryo. Dev. Cell *36*, 117–126.

Chang, K.Y., Woo, D., Jung, H., Lee, S., Kim, S., Won, J., Kyung, T., Park, H., Kim, N., Yang, H.W., et al. (2014). Light-inducible receptor tyrosine kinases that regulate neurotrophin signalling. Nat. Commun. *5*, 4057.

Chao, M.V. (2003). Neurotrophins and their receptors: a convergence point for many signalling pathways. Nat. Rev. Neurosci. *4*, 299–309.

Chen, S., Weitemier, A.Z., Zeng, X., He, L.M., Wang, X.Y., Tao, Y.Q., Huang, A.J.Y., Hashimotodani, Y., Kano, M., Iwasaki, H., et al. (2018). Near-infrared deep brain stimulation via upconversion nanoparticle-mediated optogenetics. Science *359*, 679–683.

Colombo, E., Romaggi, S., Medico, E., Menon, R., Mora, M., Falcone, C., Lochmuller, H., Confalonieri, P., Mantegazza, R., Morandi, L., et al. (2011). Human neurotrophin receptor p75NTR defines differentiation-oriented skeletal muscle precursor cells: implications for muscle regeneration. J. Neuropathol. Exp. Neurol. *70*, 133–142.

Covaceuszach, S., Konarev, P.V., Cassetta, A., Paoletti, F., Svergun, D.I., Lamba, D., and Cattaneo, A. (2015). The conundrum of the high-affinity NGF binding site formation unveiled? Biophys. J. *108*, 687–697.

Dechant, G., and Barde, Y.A. (2002). The neurotrophin receptor p75(NTR): novel functions and implications for diseases of the nervous system. Nat. Neurosci. *5*, 1131–1136.

Deshmukh, M., and Johnson, E.M., Jr. (1997). Programmed cell death in neurons: focus on the pathway of nerve growth factor deprivation-induced death of sympathetic neurons. Mol. Pharmacol. *51*, 897–906.

Green, S.H., Rydel, R.E., Connolly, J.L., and Greene, L.A. (1986). Pc12-cell mutants that possess low-affinity but not high-affinity nerve growth-factor receptors neither respond to nor internalize nerve growth-factor. J. Cell Biol. *102*, 830–843.

Grimes, M.L., Zhou, J., Beattie, E.C., Yuen, E.C., Hall, D.E., Valletta, J.S., Topp, K.S., LaVail, J.H., Bunnett, N.W., and Mobley, W.C. (1996). Endocytosis of activated TrkA: evidence that nerve growth factor induces formation of signaling endosomes. J. Neurosci. *16*, 7950–7964.

Grusch, M., Schelch, K., Riedler, R., Reichhart, E., Differ, C., Berger, W., Ingles-Prieto, A., and Janovjak, H. (2014). Spatio-temporally precise activation of engineered receptor tyrosine kinases by light. EMBO J. *33*, 1713–1726.

Guglielmi, G., Barry, J.D., Huber, W., and De Renzis, S. (2015). An optogenetic method to modulate cell contractility during tissue morphogenesis. Dev. Cell *35*, 646–660.

Hartman, D.S., McCormack, M., Schubenel, R., and Hertel, C. (1992). Multiple trkA proteins in PC12 cells bind NGF with a slow association rate. J. Biol. Chem. *267*, 24516–24522.

He, L., Zhang, Y., Ma, G., Tan, P., Li, Z., Zang, S., Wu, X., Jing, J., Fang, S., Zhou, L., et al. (2015). Near-infrared photoactivatable control of Ca(2+) signaling and optogenetic immunomodulation. Elife *4*, https://doi.org/10.7554/eLife.10024.

Hirose, M., Kuroda, Y., and Murata, E. (2016). NGF/TrkA signaling as a therapeutic target for pain. Pain Pract. *16*, 175–182.

Huang, C., Zhou, J., Feng, A.K., Lynch, C.C., Klumperman, J., DeArmond, S.J., and Mobley, W.C. (1999). Nerve growth factor signaling in caveolae-like domains at the plasma membrane. J. Biol. Chem. *274*, 36707–36714.

Huang, E.J., and Reichardt, L.F. (2001). Neurotrophins: roles in neuronal development and function. Annu. Rev. Neurosci. *24*, 677–736.

Huang, K., Dou, Q.Q., and Loh, X.J. (2016). Nanomaterial mediated optogenetics: opportunities and challenges. RSC Adv. *6*, 60896–60906.

Jensen, E.C. (2013). Quantitative analysis of histological staining and fluorescence using ImageJ. Anat. Rec. (Hoboken) *296*, 378–381.

Johnson, H.E., Goyal, Y., Pannucci, N.L., Schupbach, T., Shvartsman, S.Y., and Toettcher, J.E. (2017). The spatiotemporal limits of developmental Erk signaling. Dev. Cell *40*, 185–192.

Khamo, J.S., Krishnamurthy, V.V., Sharum, S.R., Mondal, P., and Zhang, K. (2017). Applications of optobiology in intact cells and multicellular organisms. J. Mol. Biol. *429*, 2999–3017.

Kim, B., and Lin, M.Z. (2013). Optobiology: optical control of biological processes via protein engineering. Biochem. Soc. Trans. *41*, 1183–1188.

Konermann, S., Brigham, M.D., Trevino, A., Hsu, P.D., Heidenreich, M., Cong, L., Platt, R.J., Scott, D.A., Church, G.M., and Zhang, F. (2013). Optical control of mammalian endogenous transcription and epigenetic states. Nature *500*, 472–476.

Krishnamurthy, V.V., Khamo, J.S., Mei, W., Turgeon, A.J., Ashraf, H.M., Mondal, P., Patel, D.B., Risner, N., Cho, E.E., Yang, J., et al. (2016). Reversible optogenetic control of kinase activity during differentiation and embryonic development. Development *143*, 4085–4094.

Kyung, T., Lee, S., Kim, J.E., Cho, T., Park, H., Jeong, Y.M., Kim, D., Shin, A., Kim, S., Baek, J., et al. (2015). Optogenetic control of endogenous Ca(2+) channels in vivo. Nat. Biotechnol. *33*, 1092–1096.

Lee, D., Creed, M., Jung, K., Stefanelli, T., Wendler, D.J., Oh, W.C., Mignocchi, N.L., Luscher, C., and Kwon, H.B. (2017). Temporally precise labeling and control of neuromodulatory circuits in the mammalian brain. Nat. Methods *14*, 495–503.

Lee, K.F., Li, E., Huber, L.J., Landis, S.C., Sharpe, A.H., Chao, M.V., and Jaenisch, R. (1992). Targeted mutation of the gene encoding the low affinity NGF receptor p75 leads to deficits in the peripheral sensory nervous system. Cell *69*, 737–749.

Lee, R., Kermani, P., Teng, K.K., and Hempstead, B.L. (2001). Regulation of cell survival by secreted proneurotrophins. Science *294*, 1945–1948.

Liebl, D.J., Klesse, L.J., Tessarollo, L., Wohlman, T., and Parada, L.F. (2000). Loss of brain-derived neurotrophic factor-dependent neural crest-derived sensory neurons in neurotrophin-4 mutant mice. Proc. Natl. Acad. Sci. U S A *97*, 2297–2302.

Liu, Y.S., Shreder, K.R., Gai, W.Z., Corral, S., Ferris, D.K., and Rosenblum, J.S. (2005). Wortmannin, a widely used phosphoinositide 3-kinase inhibitor, also potently inhibits mammalian polo-like kinase. Chem. Biol. *12*, 99–107.

Lomen-Hoerth, C., and Shooter, E.M. (1995). Widespread neurotrophin receptor expression in the immune system and other nonneuronal rat tissues. J. Neurochem. *64*, 1780–1789.

Lu, B., Pang, P.T., and Woo, N.H. (2005). The yin and yang of neurotrophin action. Nat. Rev. Neurosci. *6*, 603–614.

Martin, K.J., Shpiro, N., Traynor, R., Elliott, M., and Arthur, J.S. (2011). Comparison of the specificity of Trk inhibitors in recombinant and neuronal assays. Neuropharmacology *61*, 148–155.

Mauro, A., Ciccarelli, C., De Cesaris, P., Scoglio, A., Bouche, M., Molinaro, M., Aquino, A., and Zani, B.M. (2002). PKC alpha-mediated ERK, JNK and p38 activation regulates the myogenic program in human rhabdomyosarcoma cells. J. Cell Sci. *115*, 3587–3599.

Muller, K., Naumann, S., Weber, W., and Zurbriggen, M.D. (2014). Optogenetics for gene expression in mammalian cells. Biol. Chem. *396*, 145–152.

Obermeier, A., Bradshaw, R.A., Seedorf, K., Choidas, A., Schlessinger, J., and Ullrich, A. (1994). Neuronal differentiation signals are controlled by nerve growth factor receptor/Trk binding sites for SHC and PLC gamma. EMBO J. *13*, 1585–1590.

Passino, M.A., Adams, R.A., Sikorski, S.L., and Akassoglou, K. (2007). Regulation of hepatic stellate cell differentiation by the neurotrophin receptor p75NTR. Science *315*, 1853–1856.

Poo, M.M. (2001). Neurotrophins as synaptic modulators. Nat. Rev. Neurosci. *2*, 24–32.

Reade, A., Motta-Mena, L.B., Gardner, K.H., Stainier, D.Y., Weiner, O.D., and Woo, S. (2016). TAEL: a zebrafish-optimized optogenetic gene expression system with fine spatial and temporal control. Development *144*, 345–355.

Saka, Y., Hagemann, A.I., Piepenburg, O., and Smith, J.C. (2007). Nuclear accumulation of Smad complexes occurs only after the midblastula transition in *Xenopus*. Development *134*, 4209–4218.

Segal, R.A. (2003). Selectivity in neurotrophin signaling: theme and variations. Annu. Rev. Neurosci. *26*, 299–330.

Shyu, Y.J., Liu, H., Deng, X., and Hu, C.D. (2006). Identification of new fluorescent protein fragments for bimolecular fluorescence complementation analysis under physiological conditions. Biotechniques *40*, 61–66.

Stephens, R.M., Loeb, D.M., Copeland, T.D., Pawson, T., Greene, L.A., and Kaplan, D.R. (1994). Trk receptors use redundant signal-transduction pathways involving Shc and Plc-Gamma-1 to mediate Ngf responses. Neuron *12*, 691–705.

Susen, K., Heumann, R., and Blochl, A. (1999). Nerve growth factor stimulates MAPK via the low affinity receptor p75(LNTR). FEBS Lett. *463*, 231–234.

Tischer, D., and Weiner, O.D. (2014). Illuminating cell signalling with optogenetic tools. Nat. Rev. Mol. Cell Biol. *15*, 551–558.

Toettcher, J.E., Gong, D.Q., Lim, W.A., and Weiner, O.D. (2011). Light control of plasma membrane recruitment using the Phy-Pif system. Methods Enzymol. *497*, 409–423.

Tucker, C.L. (2012). Manipulating cellular processes using optical control of protein-protein interactions. Prog. Brain Res. *196*, 95–117.

Ueda, Y., Hirai, S., Osada, S., Suzuki, A., Mizuno, K., and Ohno, S. (1996). Protein kinase C activates the MEK-ERK pathway in a manner independent of Ras and dependent on Raf. J. Biol. Chem. *271*, 23512–23519.

Wang, L., Liang, Z., and Li, G. (2011). Rab22 controls NGF signaling and neurite outgrowth in PC12 cells. Mol. Biol. Cell *22*, 3853–3860.

Wang, W., Wildes, C.P., Pattarabanjird, T., Sanchez, M.I., Glober, G.F., Matthews, G.A., Tye, K.M., and Ting, A.Y. (2017). A light- and calcium-gated transcription factor for imaging and manipulating activated neurons. Nat. Biotechnol. *35*, 864–871.

Wehrman, T., He, X.L., Raab, B., Dukipatti, A., Blau, H., and Garcia, K.C. (2007). Structural and mechanistic insights into nerve growth factor interactions with the TrkA and p75 receptors. Neuron *53*, 25–38.

Widenfalk, J., Lundstromer, K., Jubran, M., Brene, S., and Olson, L. (2001). Neurotrophic factors and receptors in the immature and adult

spinal cord after mechanical injury or kainic acid. J. Neurosci. *21*, 3457–3475.

Zhang, K., and Cui, B. (2015). Optogenetic control of intracellular signaling pathways. Trends Biotechnol. *33*, 92–100.

Zhang, K., Fishel Ben Kenan, R., Osakada, Y., Xu, W., Sinit, R.S., Chen, L., Zhao, X., Chen, J.Y., Cui, B., and Wu, C. (2013). Defective axonal transport of Rab7 GTPase results in dysregulated trophic signaling. J. Neurosci. *33*, 7451–7462.

Zhang, Y., Huang, L., Li, Z., Ma, G., Zhou, Y., and Han, G. (2016). Illuminating cell signaling with near-infrared light-responsive nanomaterials. ACS Nano *10*, 3881–3885.

Zhou, X.X., Chung, H.K., Lam, A.J., and Lin, M.Z. (2012). Optical control of protein activity by fluorescent protein domains. Science *338*, 810–814.

Zoltowski, B.D., and Gardner, K.H. (2011). Tripping the light fantastic: blue-light photoreceptors as examples of environmentally modulated protein-protein interactions. Biochemistry *50*, 4–16.

STAR★METHODS

KEY RESOURCES TABLE

REAGENT or RESOURCE	SOURCE	IDENTIFIER
Antibodies		
Phospho-p44/42 MAPK (Erk1/2) (Thr202/Tyr204)	Cell Signaling Technology	#9101; RRID: AB_331646
p44/42 MAPK (Erk1/2)	Cell Signaling Technology	#9102; RRID: AB_330744
Phospho-PLCγ1 (Tyr783)	Cell Signaling Technology	#2821; RRID: AB_330855
PLCγ1	Cell Signaling Technology	#2822; RRID: AB_2163702
GFP (D5.1) XP	Cell Signaling Technology	#2956; RRID: AB_1196615
Anti-rabbit IgG, HRP-linked Antibody	Cell Signaling Technology	#7074; RRID: AB_2099233
NGF	Cell Signaling Technology	#5221
Bacterial and Virus Strains		
DH5α competent cells	Cell media facility at UIUC	N/A
Stellar™ Competent Cells	Takara Bio	#636763
Biological Samples		
Phusion DNA polymerase master mix	New England Biolabs	#M0531
In-Fusion HD Cloning Plus kit	Takara Bio	#638909
BamHI	Thermo Fisher Scientific	#FD0054
NheI	Thermo Fisher Scientific	#FD0973
F12K cell media	Gibco	#21127-022
Horse serum	Gibco	#26050-088
Fetal bovine serum	Sigma-Aldrich	#12303C
protein standards	Bio-Rad	#1610374
Chemicals, Peptides, and Recombinant Proteins		
Turbofect	Thermo Fisher Scientific	#R0533
Protease and Phosphatase Inhibitor	Thermo Fisher Scientific	#A32959
Pierce™ Coomassie Plus (Bradford) Assay Reagent	Thermo Fisher Scientific	#23238
Penicillin-Streptomycin	Corning	#30-002-CI
DPBS	Corning	#21-031-CV
RIPA lysis buffer	Millipore	#20-188
LDS sample buffer	Invitrogen	#NP0007
Polyacrylamide gels	Bio-Rad	# 4561046
PVDF membrane	Bio-Rad	# 1620177
U73122	Tocris	#1268
GF 109203X	Tocris	#0741
Erlotinib	Selleck Chemicals	#S7786
Calcein AM	Thermo Fisher Scientific	#C3100MP
Experimental Models: Cell Lines		
PC12	Laboratory of Prof. Tobias Meyer	http://web.stanford.edu/group/meyerlab/
MDA-MB-231	Laboratory of Prof. Jun-Lin Guan	https://med.uc.edu/cancerbiology/about/chair
HEK293T	Laboratory of Prof. Lin-Feng Chen	http://www.med.illinois.edu/comresearch/researchers/chenlab/
Recombinant DNA		
Lyn-TrkAICD-AuLOV-GFP (WT ICD)	This paper	N/A
Lyn-TrkAICD-GFP (No AuLOV)	This paper	N/A
Lyn-TrkAICD(Y490F)-AuLOV-GFP (Y490F)	This paper	N/A
Lyn-TrkAICD(Y490F)-AuLOV-GFP (Y785F)	This paper	N/A
Lyn-TrkAICD(Y490F)-AuLOV-GFP (Y490/785F)	This paper	N/A

(*Continued on next page*)

Continued

REAGENT or RESOURCE	SOURCE	IDENTIFIER
Lyn-TrkAICD-AuLOV-VN	This paper	N/A
Lyn-TrkAICD-AuLOV-VC	This paper	N/A
Lyn-TrkAICD-VN	This paper	N/A
Lyn-TrkAICD-VC	This paper	N/A
Software and Algorithms		
ImageJ	NIH	https://imagej.nih.gov/ij/download.html
Nikon Elements	Nikon	https://www.nikoninstruments.com/Products/Software/NIS-Elements-Advanced-Research/NIS-Elements-Viewer

CONTACT FOR REAGENT AND RESOURCE SHARING

Further information and requests for resources should be directed to and will be fulfilled by the Lead Contact, Kai Zhang (kaizkaiz@illinois.edu).

EXPERIMENTAL MODEL AND SUBJECT DETAILS

Cell Culture

PC12 cells were cultured in F12K medium supplemented with 15% horse serum, 2.5% FBS, and 1× Penicillin-Streptomycin solution (complete medium). HEK293T and MDA-MB-231 cells were cultured in DMEM medium supplemented with 10% FBS and 1× Penicillin-Streptomycin solution. Information about cell line sex is unavailable.

METHOD DETAILS

Materials

Phusion DNA polymerase master mix was purchased from NEB (Cat. #M0531). Oligonucleotides and gBlock Gene Fragments for cloning were purchased from IDT. In-Fusion HD Cloning Plus kit was purchased from Clontech (Cat. #638909). BamHI, NheI, Turbofect transfection reagent, protease/phosphatase inhibitors, Bradford reagent, and Calcein AM were purchased from Thermo Fisher Scientific (Cat. #FD0054, #FD0973, #R0533, #A32959, #23238, #C3100MP). F12K cell media and horse serum were purchased from Gibco (Cat. #21127-022, #26050-088). Fetal bovine serum (FBS) was purchased from Sigma-Aldrich (Cat. #12303C). Penicillin-Streptomycin solution and DPBS were purchased from Corning (Cat. #30-002-CI, #21-031-CV). RIPA lysis buffer was purchased from Millipore (Cat. #20-188). LDS sample buffer was purchased from Invitrogen (Cat. #NP0007). Polyacrylamide gels, PVDF membrane, and protein standards were purchased from Bio-Rad (Cat. # 4561046, # 1620177, # 1610374). NGF and antibodies were purchased from Cell Signaling Technology (Cat. #5221, #9101, #9102, #2821, #2822, #2956, #7074). Erlotinib was purchased from Selleck Chemicals (Cat. #S7786). U73122 and GF 109203X were purchased from Tocris (Cat. #1268, #0741).

Plasmids Construction

Lyn-TrkAICD-AuLOV-GFP was constructed by inserting a gBlock fragment coding the Lyn lipidation tag fused to the rat TrkA ICD and AuLOV (Lyn-TrkAICD-AuLOV) into a pEGFP-N1 vector (Clontech, discontinued; www.addgene.org/vector-database/2491/; linearized by NheI and BamHI digestion) using In-Fusion cloning. ICD mutants were generated using overlap extension PCR.

Cell Culture and Transfection

PC12 cells were cultured in F12K medium supplemented with 15% horse serum, 2.5% FBS, and 1× Penicillin-Streptomycin solution (complete medium). Cultures were maintained in a standard humidified incubator at 37°C with 5% CO_2. For differentiation assays, 2400 ng of DNA were combined with 7.2 μL of Turbofect in 240 μL of serum-free F12K. For western blots, 1200 ng of DNA (1200 ng No ICD construct alone or 700 ng No ICD construct + 500 ng ICD-containing construct) were combined with 3.6 μL of Turbofect in 120 μL of serum-free F12K. The transfection mixtures were incubated at room temperature for 20 minutes prior to adding to cells cultured in 35 mm dishes with 500 μL complete medium. For differentiation assays, the transfection medium was replaced with 2 mL complete medium after 3 hours of transfection to recover cells overnight. For western blots, the transfection medium was replaced with 1 mL serum-free F12K supplemented with 1× Penicillin-Streptomycin solution after 3 hours of transfection to serum-starved cells overnight.

PC12 Cell Differentiation Assay

Transfected and recovered PC12 cells were switched to F12K supplemented with 0.15% horse serum, 0.025% FBS, and 1× Penicillin-Streptomycin solution (starvation medium) immediately prior to incubating cells on a homemade blue LED light box emitting at

300 ìW/cm^2. Untransfected cells were similarly switched to starvation medium immediately prior to NGF treatment. Any inhibitors were added prior to NGF or light treatment. Cells were incubated with light for 24 or 44 hours before imaging GFP fluorescence at 10× magnification using a Leica DMI8 microscope. Untransfected cells were treated with 1 μM Calcein AM for 10 minutes before imaging. Differentiation ratios were calculated as follows:

$$\frac{\#\text{ of green fluorescing cells with neurite length longer than the cell body diameter}}{\#\text{ of green fluorescing cells}}$$

Epi-Illumination Fluorescence Live-Cell Microscopy

An epi-illumination inverted fluorescence microscope (Leica DMI8) equipped with a 10×, 100× objective (HCX PL FLUOTAR 100×/1.30 oil) and a light-emitting diode illuminator (SOLA SE II 365) transfected cells. Green fluorescence was detected using the GFP filter cube (Leica, excitation filter 472/30, dichroic mirror 495, and emission filter 520/35). Exposure time for both fluorescence channel was 200 ms.

Three-Dimensional Structured Illumination Microscopy (SIM)

A total of 2 × 10^5 MDA-MB-231 cells were seeded into a 35 mm dish containing a 14 mm coverslip 24 hours prior to transfection with WT ICD. Super-resolution images were acquired on an N-SIM Microscope (Nikon, Tokyo, Japan) equipped with solid-state lasers (405 nm and 488 nm). Light-induced WT ICD homo-association was stimulated by 405 nm, and SIM images were acquired under 488 nm excitation. The cells were exposed to continuous blue light (405 nm) for 300 seconds. SIM images were captured at the beginning and the end of illumination using an electron-multiplying charge coupled device (EMCCD) camera (iXon 897, Andor, USA). To reduce photobleaching during SIM image acquisition, laser power (488 nm) was reduced to <20% with a minimum exposure time of 200 ms for each image. Images were obtained at 512 × 512 using Z-stacks with a step size of 0.125 μm. SIM frames were deliberately spaced at 2-s intervals. SIM images were analyzed with Nikon Elements and ImageJ.

Western Blot

All transfected and serum-starved PC12 cells were treated with 10 μM Erlotinib (an EGFR inhibitor) for 5 minutes prior to illumination to further minimize baseline signaling. Cell were then illuminated for 10 minutes using a homemade blue LED light box emitting at 5 mW/cm^2. For PLCγ and PKC inhibitor experiments, cells were treated with inhibitors for 10 minutes prior to light treatment. Following illumination, cells were washed once with 1 mL cold DBPS and lysed with 100 μL cold lysis buffer (RIPA + protease/phosphatase inhibitor cocktail). Lysates were centrifuged at 17,000 RCF, 4°C for 10 minutes to pellet cell debris. Purified lysates were normalized using Bradford reagent. Normalized samples were mixed with LDS buffer and loaded onto 12% polyacrylamide gels. SDS-PAGE was performed at room temperature. Samples were transferred to PVDF membranes overnight at 30 V, 4°C. Membranes were blocked in 5% BSA/TBST for 1 hour at room temperature and probed with the primary and secondary antibodies according to company guidelines. Membranes were incubated with ECL substrate and imaged using a Bio-Rad ChemiDoc XRS chemiluminescence detector. Signal analysis was performed using ImageJ. Activity is defined as the signal ratio of phospho-target/total target. All reported activity is normalized to the "dark" activity of each tested condition.

QUANTIFICATION AND STATISTICAL ANALYSIS

The p-values were determined by performing two-tailed, unpaired t-test using the GraphPad Prism software.